magnetochemistry

MDPI

Article

Study of Structural, Magnetic, and Mossbauer Properties of $Dy_2Fe_{16}Ga_{1-x}Nb_x$ ($0.0 \leq x \leq 1.0$) Prepared via Arc Melting Process

Jiba N. Dahal [1,*], Kalangala Sikkanther Syed Ali [2] and Sanjay R. Mishra [3]

[1] Department of Science, Richmond Community High School, Richmond, VA 23222, USA
[2] Department of Science, Harmony School of Excellence, Dallas, TX 75249, USA; kssyedali@gmail.com
[3] Department of Physics, The University of Memphis, Memphis, TN 38152, USA; srmishra@memphis.edu
* Correspondence: jdahal@rvaschools.net

Abstract: Intermetallic compounds of $Dy_2Fe_{16}Ga_{1-x}Nb_x$ (x = 0.0 to 1.00) were synthesized by arc melting. Samples were investigated for structural, magnetic, and hyperfine properties using X-ray diffraction, vibration sample magnetometer, and Mossbauer spectrometer, respectively. The Rietveld analysis of room temperature X-ray diffraction data shows that all the samples were crystallized in Th_2Fe_{17} structure. The unit cell volume of alloys increased linearly with an increase in Nb content. The maximum Curie temperature Tc ~523 K for x = 0.6 sample is higher than Tc = 153 K of Dy_2Fe_{17}. The saturation magnetization decreased linearly with increasing Nb content from 61.57 emu/g for x = 0.0 to 42.46 emu/g for x = 1.0. The Mössbauer spectra and Rietveld analysis showed a small amount of $DyFe_3$ and $NbFe_2$ secondary phases at x = 1.0. The hyperfine field of $Dy_2Fe_{16}Ga_{1-x}Nb_x$ decreased while the isomer shift values increased with the Nb content. The observed increase in isomer shift may have resulted from the decrease in s electron density due to the unit cell volume expansion. The substantial increase in Tc of thus prepared intermetallic compounds is expected to have implications in magnets used for high-temperature applications.

Keywords: permanent magnetic materials; 2:17 intermetallic; Mossbauer spectroscopy; Curie temperature; X-ray diffraction; Rietveld analysis

Citation: Dahal, J.N.; Ali, K.S.S.; Mishra, S.R. Study of Structural, Magnetic, and Mossbauer Properties of $Dy_2Fe_{16}Ga_{1-x}Nb_x$ ($0.0 \leq x \leq 1.0$) Prepared via Arc Melting Process. *Magnetochemistry* **2021**, *7*, 42. https://doi.org/10.3390/magnetochemistry7030042

Academic Editor: Greg A. Brewer

Received: 24 January 2021
Accepted: 9 March 2021
Published: 16 March 2021

1. Introduction

Intermetallic compounds based on rare-earth elements (R) and 3d-transition elements (T) are important from a fundamental and a technological point of view as they possess outstanding magnetic properties because of their high saturation magnetization, *Ms*. R_2Fe_{17} (2:17) alloy has the most Fe-content among all R-iron intermetallic and hence they have the highest *Ms* in the class of intermetallic magnets. However, these compounds have relatively low Curie temperature, *Tc*. For example, *Tc* ~473 K for Gd_2Fe_{17} and 370 K for Dy_2Fe_{17}, along with low magnetic anisotropies [1]. Various strategies have been employed to address issues related to improving magnetic anisotropy, magnetization, and Curie temperature of R_2Fe_{17} compounds. Efforts in this direction include insertion of metalloids, hydrogen, nitrogen, and carbon in the R_2Fe_{17} matrix [2–5]. An improvement in the *Tc* value of Ce_2Fe_{17} [6], Gd_2Fe_{17} [7,8], Dy_2Fe_{17} [9,10], Pr_2Fe_{17} [11], Nd_2Fe_{17} [12], Er_2Fe_{17} [13], Tm_2Fe_{17} [14], Lu_2Fe_{17} [15,16], Ho_2Fe_{17} [17], Sm_2Fe_{17} [18] have been reported by adding metallic atoms like Si, Cr, Mn and metalloids like Ga on Fe sites. The substitution of non-magnetic atoms at Fe sites has been reported to increase the ferromagnetic coupling, leading to an increase in the *Tc* value [19,20] and magneto-crystalline anisotropy [9] of the compound. Improvements in the *Tc* of R_2Fe_{17} with substitution of a non-magnetic atom Ga have been reported for $Ce_2Fe_{17-x}Ga_x$ [21], $Sm_2Fe_{17-x}Ga_x$ [22] compounds, where the maximum in *Tc* ~462 K was observed for $Dy_2Fe_{16}Ga_1$ [9].

Low substitution of Ga content has been identified to increase the *Tc* of rare-earth intermetallic compound [9]. Additional phases are reported for a higher content of Ga

substitution [9]. More recently, replacing one Fe atom with one Nb atom has increased *Tc* up to 460 K for $Dy_2Fe_{16}Nb_1$ [23]. Based on these reports, we proposed studying the co-substitution of Ga and Nb in the Dy_2Fe_{17} compound to increase Tc values further. The study is critical in developing futuristic applications demanding high-temperature operation of magnets such as fast-breeder reactors, ion propulsion engines for spacecraft.

2. Experimental

The raw materials of Dy, Fe, Ga, and Nb metals with 99.9% purity were purchased from Sigma Aldrich (St. Louis, MO, USA). The parent alloys $Dy_2Fe_{16}Ga_{1-x}Nb_x$ (x = 0.0, 0.2, 0.4, 0.6, 0.8 and 1.0) with a stoichiometric amount of elements above were prepared by arc melting under a high purity argon atmosphere. A high degree of homogeneity was ensured by melting the ingots several times. The X-ray diffraction measurement was carried out with CuK_α (1.5406 Å) radiation on a Bruker (D8 Advance) X-ray diffractometer via a Vantec detector. Diffraction patterns were collected from 20°–70° with a step of 0.02 degrees. Room temperature (RT) magnetic properties were investigated using a vibrating sample magnetometer (VSM), and Curie temperature, *Tc*, was measured using Thermal Gravimetric Analysis (TGA) equipped with a permanent magnet. The RT ^{57}Fe Mössbauer spectra were collected in transmission geometry using 25 mCi ^{57}Co in Rh matrix γ-ray source (SEE Co. Mössbauer Spectrometer, Minneapolis, MN, USA). All the isomer shifts were measured relative to α-iron at RT used for calibration. The hyperfine parameters, viz. hyperfine field, *HF*, isomer shift, *IS*, and quadrupole shift, *QS*, were extracted by fitting the Mössbauer spectra using WMoss software (SEE Co. Minneapolis, MN, USA) [24].

3. Results and Discussion

Figure 1 represents the XRD patterns of $Dy_2Fe_{16}Ga_{1-x}Nb_x$ ($0.0 \leq x \leq 1.0$) samples. The spectra show that the samples had Th_2Ni_{17} structure (hexagonal, space group, $P6_3/mmc$) without any impurity; however, a small additional peak of $NbFe_2$ and $DyFe_3$ was detected for x = 1.0. The Rietveld [25] refined XRD patterns are shown in Figure 1b. The refined profile shows an excellent match between observed and calculated profiles. During the refinement process, all structural and lattice parameters, peak shift, background profile function, thermal parameters, etc., were refined until the observed profile functions matched with the calculated profile. The initial crystal structure parameter used for the refinement was adapted from Laio et al. [26]. The lattice parameters a and c of $Dy_2Fe_{16}Ga_{1-x}Nb_x$ ($0.0 \leq x \leq 1.0$) are shown in Figure 2, and the corresponding data are listed in Table 1. It is observed from Figure 2 that the unit cell volume increases with the increase in the Nb content, x. The increase in the unit cell volume is due to Nb ionic radius (~0.86 Å) is greater than the ionic radius of Ga (0.62 Å) [27]. The linear increase in the *c/a* ratio indicates that the unit cell's expansion along the *c*-axis is greater than that along the *a*-axis. Considering the fact that the *6c*(*4f*) dumbbell site is located along the *c*-axis, the *c*-axis expansion could affect the *Tc* value of the 2:17 compound [1]. The *c/a* ratio deviates at higher Nb concentrations (x = 1.0) due to the formation of secondary phases. In addition, it is observed from Table 1 that the average bond distance between each site changes with the concentration of both Nb and Ga (6c(4*f*-4*f*) ≈ 2.42 Å, 12*k*-12*k* ≈ 2.43 Å, 12*j*-12*j* = 2.46 Å). The 12*j*-12*j* sites show that both Ga and Nb prefer to stay in the same sites.

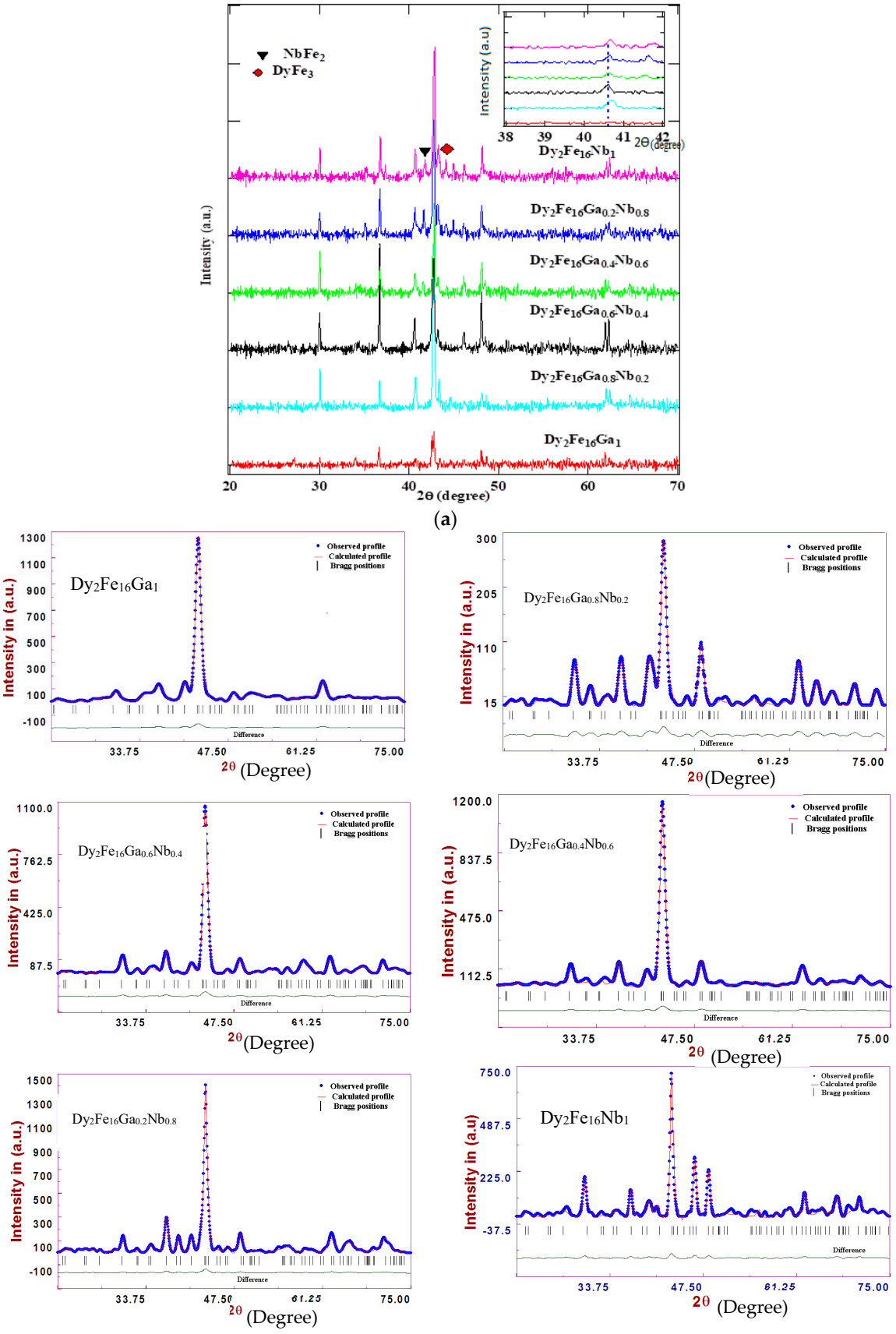

Figure 1. (**a**) X-ray diffraction patterns of $Dy_2Fe_{16}Ga_{1-x}Nb_x$ compounds. (**b**) Rietveld refinement profile for $Dy_2Fe_{16}Ga_{1-x}Nb_x$.

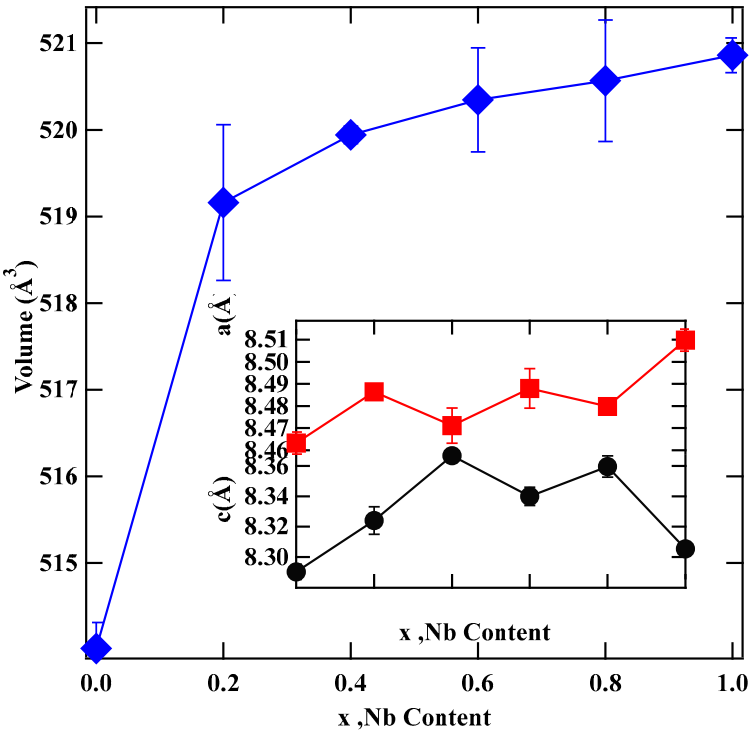

Figure 2. Lattice parameter *a* and *c* with the unit cell volume of $Dy_2Fe_{16}Ga_{1-x}Nb_x$ as a function of *x*, Nb content.

Table 1. Lattice parameters, volume, site occupancy, *Ms*, and *Tc* of $Dy_2Fe_{16}Ga_{1-x}Nb_x$.

x	*a* (Å)	*c* (Å)	*Volume* (Å^3)	*c*/*a*	6*c*(4*f*-4*f*) (Å)	6*g*-12*j* (Å)	6*g*-12*k* (Å)	12*j*-12*j* (Å)	12*k*-12*k* (Å)	*Ms* (emu/g)	*Tc* (K)
0.0	8.4632(4)	8.2902(5)	514.01(3)	0.979	2.4166(53)	2.4312(12)	2.4799(21)	2.4589(31)	2.4102(22)	61.5(7)	488(3)
0.2	8.4863(6)	8.3241(3)	519.15(9)	0.981	2.4181(22)	2.4322(18)	2.4956(8)	2.4609(27)	2.4281(32)	61.1(9)	489(5)
0.4	8.4710(8)	8.3667(8)	519.94(1)	0.988	2.4195(32)	2.4335(14)	2.5312(16)	2.4625(9)	2.4299(35)	53.2(8)	502(8)
0.6	8.4879(6)	8.3400(9)	520.34(6)	0.982	2.4286(42)	2.4344(21)	2.6901(15)	2.4656(21)	2.4325(32)	47.8(7)	523(7)
0.8	8.4798(2)	8.3596(3)	520.56(7)	0.986	2.4289(37)	2.4343(7)	2.7521(12)	2.4673(18)	2.4375(27)	44.5(9)	481(7)
1.0	8.5098(3)	8.3054(5)	520.86(2)	0.976	2.4293(4)	2.4355(21)	2.8801(23)	2.4732(32)	2.4399(29)	42.6(6)	460(6)

Figure 3 shows the room temperature *M* vs. *H* magnetization plot for $Dy_2Fe_{16}Ga_{1-x}Nb_x$. The *M* vs. *H* plot shows that the *Ms* decreases with the increase in the Nb content. The *Ms* as a function of Nb content, *x*, of $Dy_2Fe_{16}Ga_{1-x}Nb_x$ is plotted in Figure 4. From Figure 4, it is observed that the *Ms* of $Dy_2Fe_{16}Ga_{1-x}Nb_x$ decreases at the rate of −3.7 emu/g per Nb atom. The decrease in the magnetization of substituted R_2Fe_{17} compounds can be understood based on 3*d* band model. Inherently R_2Fe_{17} compounds are weak ferromagnets because both spin-up and spin-down bands are filled incompletely. The reduction in the Fe magnetic moment upon non-magnetic atom substitution results from the transfer of valence electrons of the substituted atom to the *3d* band of Fe [28,29], which progressively fills the *3d* band and moves the Fermi level up. A decrease in Fe magnetic moment is due to the electronic hybridization effect in $R_2Fe_{17}M_x$ with M = Ga, Al, and Si is well reported in the literature [30,31]. This decrease in Fe moment with the substitution is due to Fe ([Ar]3d^{6}4s^2)–Ga([Ar]4s^{2}4p^1), Fe–Al ([Ne]3s^{2}3p^1) and Fe–Si ([Ne]3s^{2}3p^2) electronic hybridizations. The decrease in the magnetic moment in Nb substituted $Dy_2Fe_{16}Ga_{1-x}Nb_x$ compound is due to indirect (3d-4s-4d) hybridization between Fe ([Ar]3d^{6}4s^2), Ga([Ar]4s^{2}4p^1), and Nb ([Kr]4d^{4}5s^1), which reduces the spin polarization of Fe-3*d* states, resulting in a net decrease in the magnetic moment. In a study reported by Lekdadri et al.; on $Co_{1-x}Nb_x$ alloy, cobalt

moment was observed to decrease with increasing Nb content in the alloys due to a similar hybridization effect [32].

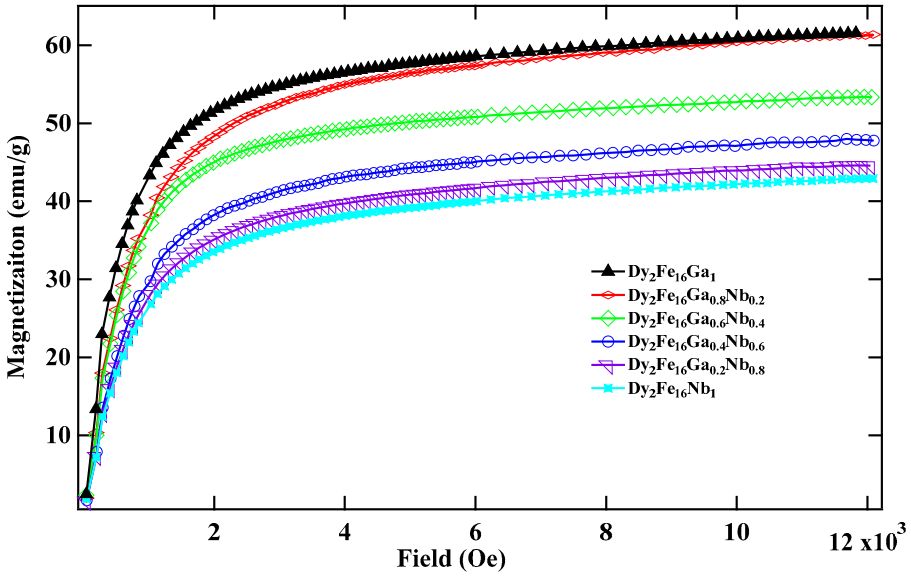

Figure 3. RT magnetization plot for $Dy_2Fe_{16}Ga_{1-x}Nb_x$.

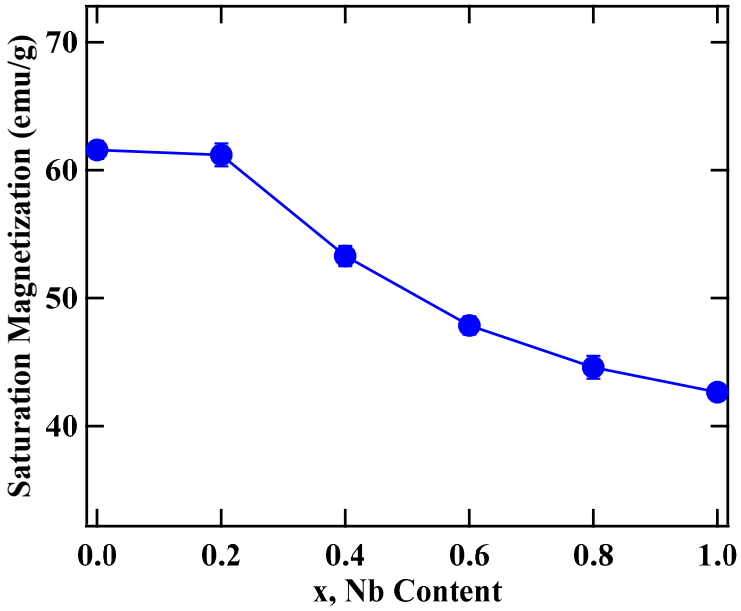

Figure 4. Room temperature (RT) saturation magnetization, *Ms*, as a function of *x*, Nb content.

The Curie temperature, *Tc*, of $Dy_2Fe_{16}Ga_{1-x}Nb_x$ as a function of Nb content is shown in Figure 5. It is observed that Curie temperature of $Dy_2Fe_{16}Ga_{1-x}Nb_x$ alloys increases with increase in Nb concentration from 488 K (x = 0.00) to a maximum of 523 K (x = 0.6) and then decreases to 460 K (x = 1.00). The achieved *Tc* for $Dy_2Fe_{16}Ga_{0.4}Nb_{0.6}$ is 35 K higher than that of $Dy_2Fe_{17}Ga_1$ and 153 K higher than that of Dy_2Fe_{17} [10]. In general, *Tc* in rare-earth intermetallic compound is due to three kinds of exchange interactions, namely the 3d-3d exchange interactions, i.e., between the magnetic moment of the Fe sub-lattice (J_{FeFe}), 4f-4f exchange interaction, i.e., the interaction between the magnetic moment within the R sub-lattice (J_{RR}), and the inter sub-lattice 3d-4f exchange interaction (J_{RFe}). It is reported that the *Tc* increases with an increase in the J_{FeFe} [33]. The interactions between the rare-earth spins (4*f*-4*f*) are assumed to be weak and negligible compared to the other

two types of interactions. Thus, the *Tc* in the R_2Fe_{17} intermetallic compound is mainly dictated by J_{FeFe}. The strength of Fe–Fe exchange interaction highly depends on interatomic Fe–Fe distance [34,35]. Accordingly, the exchange interactions between iron atoms situated at distances smaller (greater) than 2.45–2.50 Å are negative (positive). In the R_2Fe_{17}, the majority of Fe–Fe distances favor the negative interaction [9]. The negative exchange interaction can be reduced either by volume expansion or by reducing the number of Fe–Fe pairs with negative exchange interactions. The low T_C observed in the parent Dy_2Fe_{17} compound is believed to result from the antiferromagnetic coupling of Fe–Fe moments at the 6*c*(4*f*) sites [36]. Their Fe–Fe distance separation is less than 2.45 Å needed for the ferromagnetic ordering Table 1, [37]. An increase in *Tc* has been reported earlier with Ga substitution (x = 1) [9] but with a concomitant decrease in magnetization due to the magnetic dilution effect. However, the simultaneous substation of non-magnetic Ga and Nb atoms enhances the intermetallic Curie temperature without significantly lowering the saturation magnetization. It is noted from Table 1 that 4*f*-4*f* distances steadily increase with the Nb content, thus making J_{FEFe} more positive with a steady improvement in the *Tc* value.

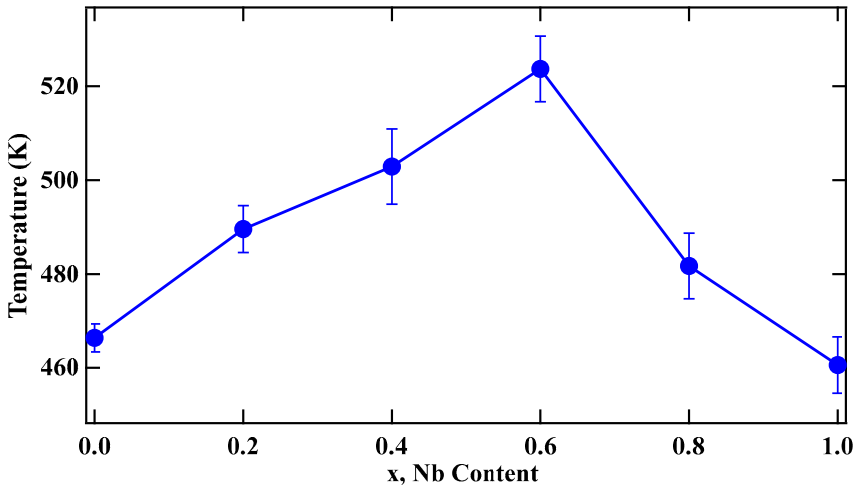

Figure 5. Curie temperature as a function of *x*, Nb content.

Figure 6 shows the room temperature fitted Mössbauer spectra for $Dy_2Fe_{16}Ga_{1-x}Nb_x$. The hyperfine parameters viz. hyperfine field, HF, and isomer shift, IS, extracted from the fits are plotted in Figure 7 and listed in Table 2. Dy_2Fe_{17} compounds have a basal magnetization that needs eight magnetic sextets to fit their Mössbauer spectra [38]. The fitting of spectra, shown in Figure 7, was carried out with eight magnetic sextets assigned to 4*f*, 6*g*, 12*j*, and 12*k* sites in Dy_2Fe_{17} [21,39–41]. The Mössbauer spectral analysis was carried out with magnetic sextets assigned to the 4*f*, 6*g*, 12*j*, and 12*k* sites in $Dy_2Fe_{17-x}Nb_x$. The 12*j* and 12*k* sites were further split into two, corresponding to the site occupancies of Fe atoms in the crystal structure of R_2Fe_{17} with planar anisotropy. The intensities of the six absorption lines of each sextet were assumed to follow the 3:2:1 intensity ratio expected for randomly oriented powder samples in zero magnetic fields, and a single common linewidth was assumed for all the seven sextets. The isomer shifts (δ) for the magnetically inequivalent sites were constrained to be the same, whereas the hyperfine fields were expected to vary at pairs of magnetically inequivalent sites due to variations in the dipolar and orbital contributions to the magnetic hyperfine fields [42]. Doublets were used for additional phases for x = 1.0 to include paramagnetic phases $DyFe_3$ and $NbFe_2$ during Mössbauer fitting. It was found that the additional doublet covered 8.86% of the area. This is in confirmation of the additional phases observed in the x-ray diffraction pattern. From Table 2, it is evident that the *HF* follows a 4*f*(6*c*) > 6*g*(9*d*) > 12*j*(18*f*) > 12*k*(18*h*) sequence, which is similar to the sequence observed in other similar RE_2Fe_{17} compounds [43,44].

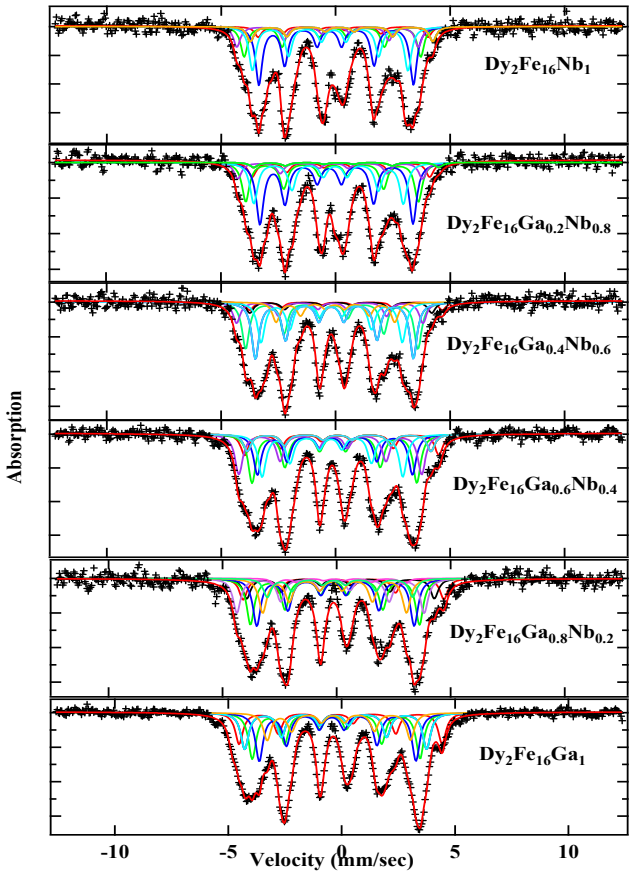

Figure 6. RT Mössbauer fitted spectra for Dy2Fe16Ga1$_{-x}$Nb$_x$.

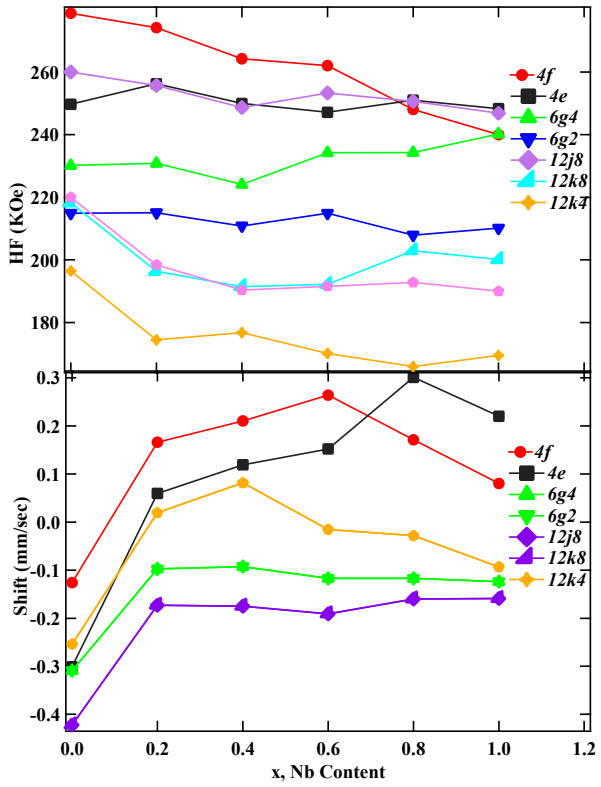

Figure 7. RT Mössbauer hyperfine parameters and isomer shift plots as a function of *x*, Nb content.

From Figure 7, it is observed that the *HF* decreases with an increase in Nb content which is in agreement with the reduction in the magnetic moment. On the other hand, the isomer shift value increases with the Nb content. The isomer shift value reflects s-electron charge density at the Fe nucleus. With the unit cell volume expansion upon Nb substitution, the *s*-electron charge density at the Fe nucleus decreases, resulting in a concomitant increase in the isomer shift value.

Table 2. The RT hyperfine parameters, hyperfine field (*HF*) (kOe), isomer shift (*IS*) (mm/s), quadrupole shift (*QS*) (mm/s), and area (%) of the Dy2Fe16Ga1$_{-x}$Nb$_x$.

	x	**4*f***	**4*e***	**6*g*1**	**6*g*2**	**12*j*1**	**12*j*2**	**12*k*1**	**12*k*2**	***Doublet***
HF (kOe)	0.0	278.7	249.7	230.1	214.9	260.0	218.1	196.4	220.0	
	0.2	274.1	256.2	230.8	215.0	255.7	196.3	174.4	198.4	
	0.4	264.2	250.0	224.1	210.8	248.6	191.4	176.7	190.3	
	0.6	262.0	247.1	234.2	214.8	253.3	192.1	170.1	191.5	
	0.8	248.0	251.01	234.2	207.9	250.6	202.9	165.9	192.7	
	1.0	240.0	248.2	240.2	210.1	246.8	200.1	169.4	190.0	19.5
IS (mm/s)	0.0	−0.126	−0.301	−0.309	−0.309	−0.422	−0.422	−0.254	−0.254	
	0.2	0.166	0.059	−0.097	−0.0975	−0.173	−0.173	0.019	0.019	
	0.4	0.210	0.119	−0.092	−0.092	−0.175	−0.175	0.081	0.081	
	0.6	0.264	0.152	−0.117	−0.117	−0.191	−0.191	−0.015	−0.015	
	0.8	0.171	0.301	−0.117	−0.117	−0.16	−0.160	−0.028	−0.028	
	1.0	0.080	0.220	−0.124	−0.124	−0.159	−0.159	−0.093	−0.093	−0.211
QS (mm/s)	0	0.158	0.010	0.133	0.259	−0.418	−0.48	0.259	−0.58	
	0.2	0.27	0.216	0.04683	0.088	−0.198	0.166	0.246	0.264	
	0.4	0.206	0.060	0.07976	0.124	−0.119	0.080	0.200	0.153	
	0.6	0.384	0.154	−0.0932	0.137	−0.129	0.046	0.024	0.156	
	0.8	0.320	0.33	−0.0683	0.313	−0.156	−0.286	0.102	0.190	
	1.0	0.420	0.081	−0.0349	0.297	−0.381	−0.153	0.039	0.089	0.035
Area (%)	0.0	13.70	14.90	20.00	21.00	10.53	5.59	10.9	3.93	
	0.2	9.14	8.68	19.63	20.24	15.74	15.82	2.39	8.25	
	0.4	8.55	5.92	18.46	20.00	16.12	15.05	5.87	9.66	
	0.6	3.42	4.64	19.73	22.70	8.92	15.96	8.43	15.93	
	0.8	6.33	2.14	17.02	26.60	7.15	14.83	10.8	15.24	
	1.0	4.27	6.02	12.14	26.80	8.22	17.75	8.46	16.42	8.86

4. Conclusions

In the present study, single phase $Dy_2Fe_{16}Ga_{1-x}Nb_x$ intermetallics were successfully synthesized using arc melting. The X-ray powder diffraction (XRD) results and the Rietveld refinements show that the samples have a Th_2Ni_{17}-type structure (space group, $P6_3/mmc$). The XRD patterns show the presence of impurities phases $DyFe_3$ and $NbFe_2$ at higher Nb content ($x > 0.80$) only, which is also confirmed by Mossbauer spectral analysis. Rietveld analysis shows a linear unit-cell volume expansion with increasing Nb content. The reduction in *Ms* of $Dy_2Fe_{16}Ga_{1-x}Nb_x$ at 300 K with an increase in Nb content is attributed to the hybridization effect. For $Dy_2Fe_{16}Ga_{0.4}Nb_{0.6}$, maximum *Tc* was observed to 523 K, which is 35 K higher than the $Dy_2Fe_{16}Ga$ compound and 153 K more elevated than its parent compound Dy_2Fe_{17}. The hyperfine fields, *HF*, of $Dy_2Fe_{16}Ga_{1-x}Nb_x$ decreased upon Nb substitution, reflecting moment reduction. The enhancement in the Curie temperature of thus prepared $Dy_2Fe_{16}Ga_{1-x}Nb_x$ compound with a judicious choice of Ga and Nb content can be helpful in areas demanding the high-temperature operation of magnets.

Author Contributions: Data Curation, Conceptual ion, Methodology and writing original draft preparation, formal analysis, investigation, visualization, J.N.D.; Revising/Editing the original draft, validation, resources, S.R.M.; Rietveld analysis, reviewing and editing, K.S.S.A. All authors have read and agreed to the published version of the manuscript.

Funding: This research received no external funding.

Institutional Review Board Statement: The study did not involve humans or animals.

Acknowledgments: The authors would like to acknowledge NSF-CMMI (Grant#: 1029780) for financially supporting this work.

Conflicts of Interest: The authors declare no conflict of interest.

References

1. Strnat, K.J. Chapter 2—Rare earth-cobalt permanent magnets. In *Handbook of Ferromagnetic Materials*; Elsevier: Amsterdam, The Netherlands, 1988; Volume 4, pp. 131–209.
2. Isnard, O.; Miraglia, S.; Soubeyroux, J.L.; Fruchart, D. Neutron powder diffraction study of $R_2Fe_{17}H_x$ compounds with R = Pr and Nd. *Solid State Commun.* **1992**, *81*, 13–19. [CrossRef]
3. Hautot, D.; Long, G.J.; Grandjean, F.; Isnard, O.; Miraglia, S. Hydrogen dynamics in the hydrides of Pr_2Fe_{17} as revealed by Mössbauer spectroscopy. *J. Appl. Phys.* **1999**, *86*, 2200–2207. [CrossRef]
4. Grandjean, F.; Long, G.J.; Mishra, S.; Pringle, O.A.; Isnard, O.; Miraglia, S.; Fruchart, D. A Mössbauer effect study of the interstitial hydrides and nitride of Nd_2Fe_{17}. *Hyperfine Interact.* **1995**, *95*, 277–289. [CrossRef]
5. Hautot, D.; Long, G.J.; Grandjean, F.; Isnard, O.; Fruchart, D. An ^{57}Fe Mössbauer spectral study of $Gd_2Fe_{17}H_x$ (for x = 0, 3, and 5) and $Sm_2Fe_{17}D_5$. *J. Magn. Magn. Mater.* **1999**, *202*, 107–118. [CrossRef]
6. Long, G.J.; Marasinghe, G.K.; Mishra, S.; Pringle, O.A.; Hu, Z.; Yelon, W.B.; Middleton, D.P.; Buschow, K.H.J.; Grandjean, F. A Magnetic, Neutron Diffraction, and Mössbauer Spectral Study of the $Nd_2Fe_{17-x}Al_x$ Solid Solutions. *J. Appl. Phys.* **1994**, *76*, 5383–5393. [CrossRef]
7. Kokorina, E.; Medvedev, M.V.; Nekrasov, I. Ab Initio Exchange Interactions and Magnetic Properties of Intermetallic Compound $Gd_2Fe_{17-x}Ga_x$. *Solid State Phenom.* **2011**, *168–169*, 196–199.
8. Dahal, J.N.; Ali, K.S.; Mishra, S.R.; Alam, J. Structural, Magnetic, and Mössbauer Studies of Transition Metal-Doped $Gd_2Fe_{16}Ga_{0.5}TM_{0.5}$ Intermetallic Compounds (TM = Cr, Mn, Co, Ni, Cu, and Zn). *J. Magnetochem.* **2018**, *4*, 54. [CrossRef]
9. Shen, B.-G.; Cheng, Z.-H.; Gong, H.-Y.; Liang, B.; Yan, Q.-W.; Zhan, W.-S. Magnetic anisotropy of $Dy_2Fe_{17-x}Ga_x$ compounds. *Solid State Commun.* **1995**, *95*, 813–816. [CrossRef]
10. Dahal, J.N.; Ali, K.S.; Mishra, S.R.; Neupane, D. Effect of Ga and Zr Substitution on the Properties of $Dy_2Fe_{17-X}Zr_X$ and $Dy_2Fe_{16}Ga_{1-x}Zr_x$ ($0 \leq x \leq 1$) Intermetallic Compounds Prepared via Arc Melting Process. *J. Magnetochem.* **2020**, *6*, 9. [CrossRef]
11. Gorria, P.; Alvarez, P.; Marcos, J.S.; Llamazares, J.L.S.; Parez, M.J.; Blanco, J.A. Crystal structure, magnetocaloric effect and magnetovolume anomalies in nanostructured Pr_2Fe_{17}. *Acta Mater.* **2009**, *57*, 1724–1733. [CrossRef]
12. Isnard, O.; Guillot, M. Investigation of magnetic properties of Nd_2Fe_{17} and $Nd_2Fe_{17}H_x$ in high magnetic field. *J. Appl. Phys.* **2000**, *86*, 5326–5328. [CrossRef]
13. Grandjean, F.; Isnard, O.; Hautot, D.; Long, G.J. A structural, magnetic, and Mössbauer spectral study of Er_2Fe_{17} and hydrides. *Phys. Rev. B* **2000**, *63*, 144061. [CrossRef]
14. Hao, Y.; Zhang, X.; Wang, B.; Yuang, Y.; Wang, F. Anomalous thermal expansion and magnetic properties of $Tm_2Fe_{17-x}Cr_x$ compounds. *J. Appl. Phys.* **2010**, *108*, 023915. [CrossRef]
15. Kunchin, A.; Iwasieczko, W. Enhancement of the magnetocaloric effect in the $Lu_2Fe_{17-x}Mn_x$ system. *Solid State Commun.* **2010**, *150*, 1580–1583. [CrossRef]
16. Arnold, Z.; Kunchin, A.; Kamarad, J. Instability of the ferromagnetic ground state in $Lu_2Fe_{17-x}M_x$[x = 0.5, 0.7]. *J. Appl. Phys.* **2012**, *111*, 07E310. [CrossRef]
17. Wang, F.; Shen, B.-G.; Zhang, P.; Cheng, Z.-H.; Zhang, J.; Gong, H.; Liang, B.; Sun, X.; Yan, Q. Effect of Ga substitution on the structure and magnetic properties of $Ho_2Fe_{17-x}Ga_x$ (x = 0–8) compounds. *J. Appl. Phys.* **1998**, *83*, 3250–3255. [CrossRef]
18. Wang, Z.; Dunlap, R.A. Effects of Al substitutions on the magnetic anisotropy of Sm_2Fe_{17} compounds. *J. Phys. Condens. Matter* **1993**, *5*, 1407–1414. [CrossRef]
19. Li, D.; Zhang, J.; Dowben, P.A.; Garrison, K. Evidence for imperfect ferromagnetic coupling between the Gd(0001) surface and the bulk. *J. Phys. Condens. Matter* **1993**, *5*, L73. [CrossRef]
20. Wang, Z.; Dunlap, R.A. Investigation of the hard-magnetic properties of Sm_2Fe_{17} compounds with Ga substitution. *Philos. Mag. B* **1994**, *69*, 103–111. [CrossRef]
21. Long, G.J.; Mishra, S.R.; Pringle, O.A.; Yelon, W.B.; Hu, Z.; Grandjean, F.; Middleton, D.P.; Buschow, K.H.J. A magnetic, neutron diffraction and Mossbauer spectral study of the $Ce_2Fe_{17-x}Ga_x$ solid solution. *J. Magn. Magn. Mater.* **1997**, *176*, 217–232. [CrossRef]
22. Zhang, Y.; Budnick, J.I.; Hines, W.A.; Shen, B.G.; Cheng, Z. Effect of Ga substitution on the Sm sublattice anisotropy in $Sm_2Fe_{17-x}Ga_x$ ($0 < x < 8$). *J. Appl. Phys.* **1999**, *85*, 4663–4665.
23. Rai, B.; Ali, K.S.; Mishra, S.; Khanra, S.; Ghosh, K. A structural, magnetic and Mossbauer study of the $Dy_2Fe_{17-x}Nb_x$ solid solutions. *J. Magn. Magn. Mater.* **2014**, *353*, 51–56. [CrossRef]
24. Kent, T.A. *Wmoss Mossbauer Spectral Analysis Software*; Report; WEB Research Co.: Edmonton, AB, Canada, 1993.
25. Rietveld, H.M. A profile refinement method for nuclear and magnetic structures. *J. Appl. Cryst.* **1969**, *2*, 65. [CrossRef]
26. Liao, L.X.; Altounican, Z.; Ryan, D.H. Cobalt site preferences in iron rare-earth-based compounds. *Phy. Rev. B* **1993**, *47*, 11230. [CrossRef] [PubMed]

27. Ulyanov, A.N.; Kim, J.S.; Shin, G.M.; Song, K.J.; Kang, Y.M.; Yoo, S.I. $La_{0:7}Ca_{0:3}Mn_{0:95}M_{0:05}O_3$ manganites (M = Al, Ga, Fe, Mn, and In):Local structure and electron configuration effect on Curie temperature and magnetization. *Phys. B Condens. Matter* **2007**, *388*, 16–19. [CrossRef]
28. Suresh, K.G.; Rama Rao, K.V.S. Fe 57 Mossbauer investigation on $(Er,Pr)_2(Fe,Al)_{17}$ compounds and their nitrides. *Phys. Rev. B* **1997**, *55*, 15060. [CrossRef]
29. Hu, B.P.; Li, H.S.; Sun, H.; Coey, J.M.D. A ^{5}e Mossbauer study of a new series of rare-earth iron nitrides: $R_2Fe_{17}N_{3-}$ delta. *J. Phys. Condens. Mater.* **1991**, *3*, 3983. [CrossRef]
30. Huang, M.Z.; Ching, W.Y. Effects of Al substitution in Nd_2Fe_{17} studied by first-principles calculations. *J. Appl. Phys.* **1994**, *76*, 7046–7048. [CrossRef]
31. Huang, M.Z.; Ching, W.Y. First-principles calculation of the electronic and magnetic properties of $Nd_2Fe_{17-x}M_x$ (M = Si, Ga) solid solutions. *J. Appl. Phys.* **1996**, *79*, 5546–5549. [CrossRef]
32. Lekdadri, A.; Chami, R.; Saadi, A.; Lassri, H.; Omari, L.H. First-principle study of electronic and magnetic properties in cobalt-niobium alloys. *Mater. Today Proc.* **2021**, *37*, 3813–3820. [CrossRef]
33. Rao, K.R.; Ehrenberg, H.; Markandeyulu, G.; Varadaraju, U.; Venkatesan, M.; Suresh, K.; Murthy, V.; Schmidt, P.; Fuess, H. On the Structural and Magnetic Properties of $R_2Fe_{17-x}(A,T)_x$ (R = Rare Earth; A = Al, Si, Ga; T = Transition Metal) Compounds. *Phys. Status Solidi* **2002**, *189*, 373–388. [CrossRef]
34. Neél, L. Propriétés magnétiques de l'état métallique et énergie d'interaction entre atoms magnétiques. *Ann. Phys.* **1936**, *5*, 232. [CrossRef]
35. Li, Z.W.; Morrish, A.H. Negative exchange interactions and Curie temperatures for Sm_2Fe_{17} and $Sm_2Fe_{17}N_y$. *Phys. Rev. B* **1997**, *55*, 3670. [CrossRef]
36. Bara, J.J.; Pedziwiatr, A.T.; Zarek, W. Investigations of crystal and magnetic properties of Dy-Fe intermetallic compounds. *J. Magn. Magn. Mater.* **1982**, *27*, 168–174. [CrossRef]
37. Valeanu, M.; Plugaru, N.; Burzo, E. Effect of nitrogenation on the magnetic properties of $Y_2Fe_{17-x}M_x$ compounds, with M = Al, Ga or Si. *Solid State Commun.* **1994**, *89*, 519. [CrossRef]
38. Isnard, O.; Hautot, D.; Long, G.L.; Grandjean, F. A structural magnetic and Mossbauer spectral study of Dy_2Fe_{17} and hydrides. *J. App. Phys.* **2000**, *88*, 2750–2759. [CrossRef]
39. Buschow, K.H.J.; Wieringen, J.S.V. Crystal structure and magnetic properties of cerium-iron compounds. *Phys. Status Solidi* **1970**, *42*, 231. [CrossRef]
40. Levinson, L.M.; Rosenberg, E.; Shaulov, A.; Strnat, K. Mössbauer Study of Some 2–17 Lanthanide-Iron Compounds. *J. Appl. Phys.* **1970**, *41*, 910–912. [CrossRef]
41. Alp, E.E.; Umarji, A.M.; Malik, S.K.; Shenoy, G.K.; Huang, M.Q.; Boltich, E.B.; Wallace, W.E. ^{57}Fe Mössbauer studies on Si-substituted Er_2Fe_{17}. *J. Magn. Magn. Mater.* **1987**, *68*, 305–308. [CrossRef]
42. Wang, J.L.; Campbell, S.J.; Tegus, O.; Marquina, C.; Ibarra, M.R. Magnetovolume effect and magnetic properties of $Dy_2Fe_{17-x}Mn_x$. *Phys. Rev. B* **2007**, *75*, 174423. [CrossRef]
43. Grandjean, F.; Isnard, O.; Long, G.J. Magnetic and Mössbauer spectral evidence for the suppression of the magnetic spin reorientation in Tm_2Fe_{17} by deuterium. *Phys. Rev. B* **2002**, *65*, 064429. [CrossRef]
44. Long, G.J.; Isnard, O.; Grandjean, F. A Mössbauer spectral study of the magnetic properties of Ho_2Fe_{17} and Ho_2 $Fe_{17}D_{3.8}$. *J. Appl. Phys.* **2002**, *91*, 1423–1430. [CrossRef]